

Performance Analysis of Power Spectrum Efficiency under Interference Cancellation

Kosuru Padma¹, G.Phani kumar²

^{1,2} *Electrical and Electronics Engineering Department,*

^{1,2} , bab(A), Visakhapatnam, A.P., India

Abstract: A distributed interference cancellation scheme for cellular networks is considered in which a subset of receivers forward their decoded messages to another subset of receivers. The messages can then be used to cancel interference with estimated cross-channel gains. A distributed power control algorithm is presented that harnesses the gain of interference cancellation and that takes into account channel estimation error. The algorithm is based on the exchange of interference prices, but in this case the local power updates are not concave due to nonlinear terms introduced by channel estimation errors. A partial cancellation scheme is then presented where the power updates are derived in closed form. We show that the algorithm converges to a local optimum of the weighted sum-rate maximization problem. Two methods for sorting users into the two groups that respectively forward and receive the decoded messages are presented. The first is sequential and is shown to converge to a local optimum. The second is a simple heuristic that is based on a stochastic geometric approach. Numerical results show that power control and adaptive partitioning of the users can add substantial gains to interference cancellation.

Index Terms— Distributed power control, uplink channel, coordinated multi-point, multi-cell processing, distributed interference cancellation, fractional power control, stochastic geometry, channel estimation error, interference prices.

I. INTRODUCTION

The phantom productivity of current cell systems is constrained by between cell impedance, which is relied upon to increment with more densification of the entrance arrange. A key element that is being acquainted with moderate, and indeed, even endeavour this obstruction is

participation among the transmitters and recipients in the system. Collaboration incorporates both tradings got signals for joint handling (identification) and trading messages for agreeable transmissions [1]. Such Coordinated Multi-Point (CoMP) procedures have been presented in current Fourth Generation (LTE) measures [2] and are a piece of the characterizing advances for 5G [3]. A broad review on CoMP can be found in One form of uplink cooperation is multi-cell processing (MCP) [8], [9], in which all Base Transceiver Stations (BTSs) in a cluster jointly decode their users. The improvement in spectral efficiency achieved by MCP occurs at the expense of a tremendous increase in backhaul traffic arising from the need to exchange complexvalued baseband signals received at each antenna within the cluster. This entails the need for large backhaul capacity links on the order of Gbps [10], Moreover MCP puts stringent synchronization requirements on the participating base stations, adding to the complexity of implementation[2].

We present a distributed algorithm for updating the transmit powers locally, which accounts for both interference cancellation and channel estimation error. The algorithm is proven to converge to a local optimum. Although our approach is based on the computation of interference prices the surplus functions change significantly with interference cancellation and become nonconvex. To circumvent the difficulty of maximizing such a nonconvex objective, a partial (weighted) cancellation scheme is then introduced for which the power updates are given in closed form.

We also propose an algorithm for sorting the users into the two groups A and B. A method for moving users sequentially from one group to the other to increase a sum utility objective is presented and shown to converge to a local optimum. Numerical results are presented that show that the combination of power control and adaptive user partitioning can provide substantial performance gains. We also present a simple heuristic for partitioning the users based on a random spatial model for the network topology We compare the performance of the heuristic with that of

the sequential algorithm and show that the former suffers only a small degradation in performance.

One type of uplink participation is multi-cell handling (MCP) [8], [9], in which all Base Transceiver Stations (BTSs) in a bunch mutually translate their clients. The change in ghastry proficiency accomplished by MCP happens to the detriment of an enormous increment in backhaul movement emerging from the need to trade complexvalued baseband signals got at every reception apparatus inside the bunch. This involves the requirement for extensive backhaul limit connects on the request of Gbps [10], [11]. Besides MCP puts stringent synchronization necessities on the taking part base stations, adding to the intricacy of execution [2].

An elective uplink collaboration conspire is organize or on the other hand appropriated Interference Cancelation (DIC) where a subset of recipients pass their decoded signals to different beneficiaries to cross out the related obstruction. DIC has been appeared to give throughput picks up that are near those given by MCP to direct group sizes [13], however with backhaul activity diminished by one to two requests of size. DIC can for the most part perform superior to MCP for systems with constrained backhaul and direct between cell impedance. A low multifaceted nature multicell impedance cancelation plot that locations the disentangling inertness was proposed in [14]. In this work, we propose a disseminated control calculation that can tackle the additions of DIC among the

cells. Adding power control to DIC can additionally increment the whole rate while representing distinctive needs or on the other hand utilities crosswise over clients. We demonstrate that power control plans like partial power control (FPC) utilized in LTE don't completely abuse participation. A broad study on control in remote cell frameworks conveyed calculations that expand an aggregate utility target what's more, require constrained coordination. Here we take after the general approach in characterizing obstruction costs, which are iteratively refreshed with transmit powers. Another favorable position of acquainting power control with DIC is that it can make up for channel estimation mistake, which represents an essential confinement on the execution of impedance cancelation plans For a base station to cross out the impedance from any given client, it needs to recreate that client's flag utilizing the channel appraise and the traded images. Erroneous channel gauges prompt high leftover impedance.

We consider an uplink obstruction cancelation conspire in which the cells are divided into two gatherings, An and B. All clients in the two gatherings transmit their messages at the same time. Clients in aggregate An are decoded first by their particular serving cells, subject to obstruction from every single other client in the system. The decoded images are then sent to BTSs in aggregate B for impedance cancelation. Gathering B clients are at that point decoded subject to impedance from gather B clients as it were. This

plan applies to general topologies including little cell thick access systems and HetNets

We show a dispersed calculation for refreshing the transmit controls locally, which represents both impedance cancelation and channel estimation blunder. The calculation is demonstrated to meet to a neighborhood ideal. In spite of the fact that our approach depends on the calculation of obstruction costs the surplus capacities change fundamentally with impedance cancelation and move toward becoming nonconvex. To dodge the trouble of augmenting such a nonconvex objective, a halfway (weighted) cancelation plot is then presented for which the control refreshes are given in shut shape.

We additionally propose a calculation for arranging the clients into the two gatherings An and B. A strategy for moving clients consecutively from one gathering to the next to expand a whole utility goal is exhibited and appeared to join to a nearby ideal. Numerical outcomes are exhibited that demonstrate that the mix of energy control and versatile client dividing can give generous execution picks up. We additionally exhibit a basic heuristic for dividing the clients in light of an irregular spatial model for the system topology We look at the execution of the heuristic with that of the consecutive calculation and demonstrate that the previous endures just a little debasement in execution. In the following segment, the model for DIC is presented.

The weighted whole rate expansion objective along with the fundamental optimality conditions are exhibited in Section III. The Distributed Interference Cancelation Power Control (DICPC) plot is exhibited in area IV. In segment V, fractional cancelation is presented and used to infer shut frame control refreshes. Dividing calculations are talked about in Sections VI and VII. Numerical cases are appeared in area VIII and conclusions are given in segment IX.

II. APPROPRIATED INTERFERENCE CANCELATION

Think about a cell framework (Fig. 1) comprising of cells listed from $I = 1, \dots, N$. Every cell I has a BTS that calendars numerous clients for uplink transmission, be that as it may, just a single client is distributed to a given arrangement of time frequency resource blocks.¹ We assume that the BTSs can cooperate. Namely, after the mobiles transmit their packets to their respective BTSs, every BTS, which successfully decodes its own user, passes the decoded bits to the cells with which it cooperates for the purpose of interference cancellation.

Fig. 1 shows a network of four cells where BTSs 1, 3, and 4 pass their decoded messages to BTS 2. Before cancellation the signal received at cell 2 is

$$y_2 = g_{2 \rightarrow 2}x_2 + g_{1 \rightarrow 2}x_1 + g_{3 \rightarrow 2}x_3 + g_{4 \rightarrow 2}x_4 + v_2,$$

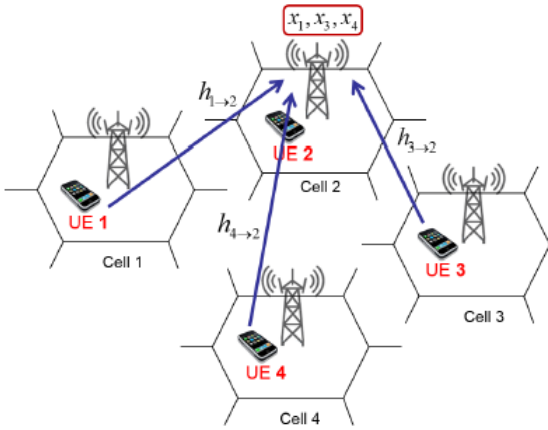


Fig. 1. BTS cooperation on the uplink.

Cell 2 has imperfect estimates of the channel gains, $g_{k \rightarrow 2}$, $k = 1, 3, 4$, which we denote by $\hat{g}_{1 \rightarrow 2}$, $\hat{g}_{3 \rightarrow 2}$, and $\hat{g}_{4 \rightarrow 2}$, respectively. After cancellation, the received signal becomes

$$y'_2 = g_{2 \rightarrow 2}x_2 + \tilde{g}_{1 \rightarrow 2}x_1 + \tilde{g}_{3 \rightarrow 2}x_3 + \tilde{g}_{4 \rightarrow 2}x_4 + v_2,$$

$$G_{i \rightarrow j} \triangleq |g_{i \rightarrow j}|^2, \quad \hat{G}_{i \rightarrow j} \triangleq E \left(|\hat{g}_{i \rightarrow j}|^2 \right),$$

$$\tilde{G}_{i \rightarrow j} \triangleq E \left(|\tilde{g}_{i \rightarrow j}|^2 \right),$$

$$I_2 = G_{1 \rightarrow 2} + G_{3 \rightarrow 2} + G_{4 \rightarrow 2} + \sigma_v^2,$$

$$I'_2 = \tilde{G}_{1 \rightarrow 2} + \tilde{G}_{3 \rightarrow 2} + \tilde{G}_{4 \rightarrow 2} + \sigma_v^2.$$

To estimate the cross-channel gains needed for cancellation, the i th user transmits N_{coh} pilots tones. We assume that those pilots are sent with the same power as data symbols (to avoid symbol to symbol power fluctuations that increase the peak-to-average power ratio of the transmitted signal and reduce the efficiency of the power amplifier), and that the channel is stationary during this period. To avoid pilot contamination, the users can *coordinate* pilot transmissions, meaning they transmit orthogonal pilot sequences.³ Fig. 2 shows a 57-cell network where we divide the cells into 7 pilot coordination clusters, each having 9 orthogonal pilot sequences. Although the base sequences across clusters are not orthogonal, they have low cross-correlations.

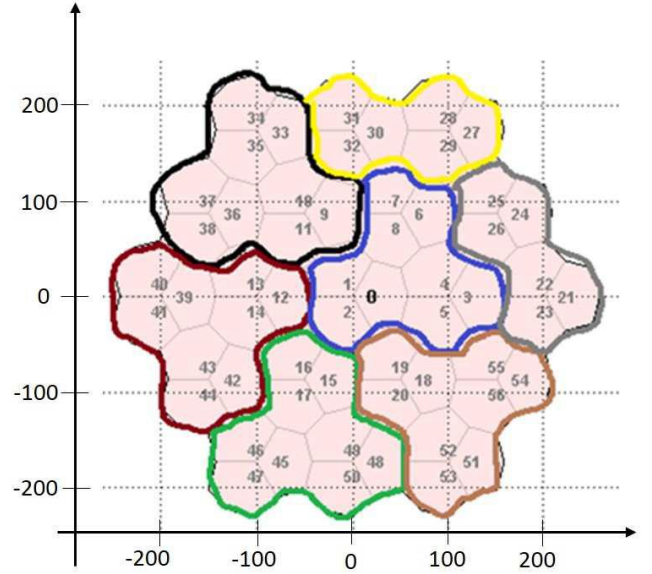


Fig. 2. Pilot-coordination clusters in a 57-cell mobile broadband network. The unit of distance is meters.

Consider the scenario where cell j is trying to estimate the gain $G_{i \rightarrow j}$ from the mobile in cell i . During mobile i 's pilot transmission, cell j sees interference from two types of cells:

1. $C(i)$, $\{k \neq i: \text{cells } k \text{ and } i \text{ coordinate pilots}\}$
2. $\bar{C}(i)$, $\{k \neq i: \text{cell } k \text{ and } i \text{ do not coordinate pilots}\}$

The signal received at cell j is then

³In the LTE uplink orthogonal sequences among users are obtained by performing cyclic shifts of a base sequence of pilots [16], where x_i is the vector of pilots sent by user i . We assume cell j obtains a Minimum Mean Squared Error (MMSE)

estimate of $g_{i \rightarrow j}$, namely,

$$\hat{g}_{i \rightarrow j} = \beta_{i \rightarrow j} \frac{x_i^H y_j}{N_{coh}},$$

$$0 \leq \beta_{i \rightarrow j} \triangleq \frac{G_{i \rightarrow j}}{G_{i \rightarrow j} + \frac{1}{N_{coh}^2} \sum_{l \in \bar{C}(i)} G_{l \rightarrow j} + \frac{\sigma_{v_j}^2}{N_{coh}}} \leq 1.$$

$$\tilde{G}_{i \rightarrow j} = E \left(|g_{i \rightarrow j} - \hat{g}_{i \rightarrow j}|^2 \right) = \frac{G_{i \rightarrow j} F_{i \rightarrow j}}{G_{i \rightarrow j} + F_{i \rightarrow j}}, \quad (4)$$

$$F_{i \rightarrow j} \triangleq \frac{1}{N_{coh}^2} \sum_{l \in \bar{C}(i)} G_{l \rightarrow j} + \frac{\sigma_{v_j}^2}{N_{coh}}. \quad (5)$$

$$\hat{g}_{i \rightarrow j} = \frac{\mathbf{x}_i^H \mathbf{y}_j}{N_{coh}}, \quad (6)$$

$$\tilde{G}_{i \rightarrow j} = F_{i \rightarrow j}. \quad (7)$$

The difference between (6) and the MMSE estimator is that the estimation error variance $\tilde{G}_{i \rightarrow j}$ in (7) is not guaranteed to be less than the channel gain $G_{i \rightarrow j}$. This implies that there can be cases where interference cancellation degrades performance. For the example shown in Fig. 1, this means that $|'2 > |2$. To address this problem, we introduce a partial cancellation scheme in section V.

III. SYSTEM MODEL

We divide the N cells in the network into two groups: A and B. The mobile users in both cell groups transmit their symbols simultaneously. Decoding of transmitted symbols happens in two stages. In the first stage, group A BTSs decode their respective users while experiencing interference from all other users in both groups A and B. In the second stage, group A BTSs pass their decoded symbols to group B BTSs for interference cancellation. One way to partition the network cells into two groups is to view group B users as premium users who are ensured a higher quality of service. In Sections VI and VII, we present partitioning methods to increase the sum rate performance metric. A BTS decoding a user equipment (UE) in cell i that belongs to group A sees interference from a BTS decoding a UE in cell k that belongs to group B sees direct interference from group B users but only residual interference from group A users, i.e., Generally, current controlled voltage source inverters are used to interface the intermittent RES in distributed system.

Recently, a few control strategies for grid connected inverters incorporating PQ solution have been proposed. In [3] an inverter operates as active inductor at a certain frequency to absorb the harmonic current. But the exact calculation of network inductance in real-time is difficult and may deteriorate the control performance. A similar approach in which a shunt active filter acts as active conductance to damp out the harmonics in distribution network is proposed in [4]. In [5], a control strategy for renewable interfacing inverter based on p-q theory is proposed. In this strategy both load and inverter current sensing is required to compensate the load current harmonics.

The non-linear load current harmonics may result in voltage harmonics and can create a serious PQ problem in the power system network. Active power filters (APF) are extensively used to compensate the load current harmonics and load

unbalance at distribution level. This results in an additional hardware cost. However, in this paper authors have incorporated the features of APF in the, conventional inverter interfacing renewable with the grid, without any additional hardware cost. Here, the main idea is the maximum utilization of inverter rating which is most of the time underutilized due to intermittent nature of RES. It is shown in this paper that the grid-interfacing inverter can effectively be utilized to perform following important functions: 1) transfer of active power harvested from the renewable resources (wind, solar, etc.); 2) load reactive power demand support; 3) current harmonics compensation at PCC; and 4) current unbalance and neutral current compensation in case of 3-phase 4-wire system.

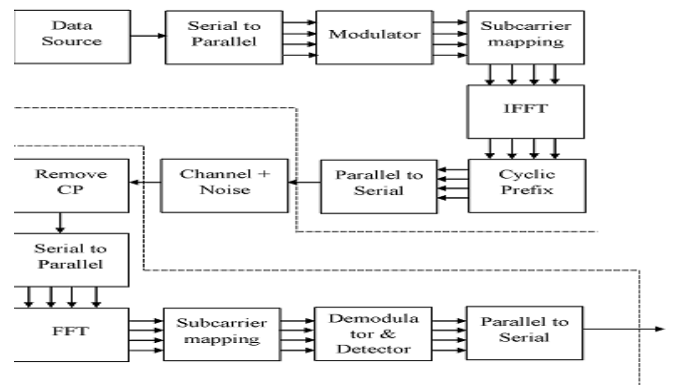


Fig3. Block diagram representation of the OFDM transceiver

Moreover, with adequate control of grid-interfacing inverter, all the four objectives can be accomplished either individually or simultaneously. The PQ constraints at the PCC can therefore be strictly maintained within the utility standards without additional hardware cost.

a) Serial to Parallel Conversion

The input serial data stream is formatted into the word size required for transmission, e.g. 2 bits/word for QPSK, and shifted into a parallel format. The data is then transmitted in parallel by assigning each data word to one carrier in the transmission.

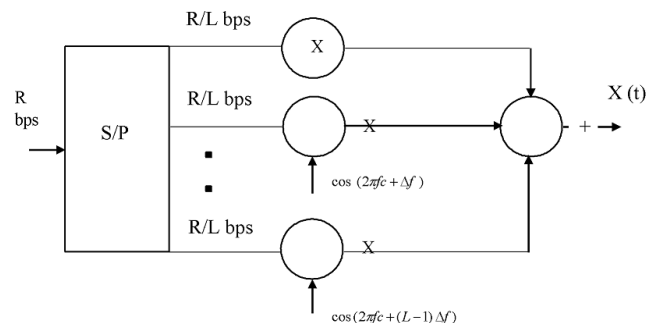


Fig 4. Serial to parallel conversion

The figure represents a serial to parallel conversion diagram.

b) Data Scrambler:

The DATA field, composed of SERVICE, PSDU, tail, and pad parts, shall be scrambled with a length-127 frame-synchronous scrambler. The octets of the PSDU are placed in the transmit serial bit stream, bit 0 first and bit 7 last. The frame synchronous scrambler uses the generator polynomial S(x) as follows, and is illustrated in Figure 3.7:

The 127-bit sequence generated repeatedly by the scrambler shall be (leftmost used first), 00001110 11110010 11001001 00000010 00100110 00101110 10110110 00001100 11010100 11100111 10110100 00101010 11111010 01010001 10111000 11111111, when the “all ones” initial state is used. The same scrambler is used to scramble transmit data and to descramble receive data. When transmitting, the initial state of the scrambler will be set to a pseudo random non-zero state. The seven LSBs of the SERVICE field will be set to all zeros prior to scrambling to enable estimation of the initial state of the scrambler in the receiver.

c) Convolutional Encoder

The DATA field, composed of SERVICE, PSDU, tail, and pad parts, shall be coded with a convolutional encoder of coding rate $R = 1/2, 2/3, \text{ or } 3/4$, corresponding to the desired data rate. The convolutional encoder shall use the industry-standard generator polynomials, $g_0 = 1338$ and $g_1 = 1718$, of rate $R = 1/2$,

The bit denoted as “A” shall be output from the encoder before the bit denoted as “B.” Higher rates are derived from it by employing “puncturing.” Puncturing is a procedure for omitting some of the encoded bits in the transmitter (thus reducing the number of transmitted bits and increasing the coding rate) and inserting a dummy “zero” metric into the convolutional decoder on the receive side in place of the omitted bits.

d) Modulation Of Data

The data to be transmitted on each carrier is then differential encoded with previous symbols, then mapped into a Phase Shift Keying (PSK) format. Since differential encoding requires an initial phase reference an extra symbol is added at the start for this purpose. The data on each symbol is then mapped to a phase angle based on the modulation method. For example, for QPSK the phase angles used are 0, 90, 180, and 270 degrees. The use of phase shift keying produces a constant amplitude signal and was chosen for its simplicity and to reduce problems with amplitude fluctuations due to fading.

e) Generation of OFDM

To generate OFDM well, relationship between all carriers must be controlled carefully in order to control the orthogonality of carriers. For this motive, OFDM is generated by 1st choosing the spectrum required, depends on data input, and scheme of modulation used. For transmission, data is assign to every produced carrier. The

required phase and amplitude of carrier is calculated and with the help of IFT converted back to its time domain. However in many applications, IFFT is used. IFFT performs the transformation efficiently.

f) Subcarrier Modulation Mapping

The OFDM subcarriers shall be modulated by using BPSK, QPSK, 16-QAM, or 64-QAM modulation, depending on the RATE requested. The encoded and interleaved binary serial input data shall be divided into groups of NBPSC (1, 2, 4, or 6) bits and converted into complex numbers representing BPSK, QPSK, 16-QAM, or 64-QAM constellation points. The conversion shall be performed according to Gray-coded constellation mappings, illustrated in Figure 116, with the input bit, b0, being the earliest in the stream. The output values, d, are formed by multiplying the resulting (I+jQ) value by a normalization factor KMOD, as described in Equation

The normalization factor, KMOD, depends on the base modulation mode, as prescribed in Table 3.1. Note that the modulation type can be different from the start to the end of the transmission, as the signal changes from SIGNAL to DATA, as shown in the frame format. The purpose of the normalization factor is to achieve the same average power for all mappings. In practical implementations, an approximate value of the normalization factor can be used, as long as the device conforms with the modulation accuracy requirements.

Table 3.1: Modulation-dependent normalization factor KMOD

Modulation	KMOD
BPSK	1
QPSK	$1/\sqrt{2}$
16-QAM	$1/\sqrt{10}$
64-QAM	$1/\sqrt{2}$

For BPSK, b0 determines the I-value, as illustrated in Table 3.2. For QPSK, b0 determines the I-value and b1 determines the Q value, as illustrated in Table 3.3. For 16-QAM, b0b1 determines the I-value and b2b3 determines the Q value, as illustrated in Table 3.4. But 8-QAM is used in this project. For 64-QAM, b0b1b2 determines the I-value and b3b4b5 determines the Q value, but it is not included here.

Table 3.2—BPSK encoding table

Input bit (b0)	I-out	Q-out
0	-1	0
1	1	0

Table 3.3—QPSK encoding table

Here b0 and b1 represents the inphase and quadrature values respectively. Here the bits b0 b1 represents the in-phase value and the bits b2 b3 represents the quadrature value.

g) *Pilot Subcarriers*

In each OFDM symbol, four of the subcarriers are dedicated to pilot signals in order to make the coherent detection robust against frequency offsets and phase noise. These pilot signals shall be put in subcarriers $-21, -7, 7$ and 21 . The pilots shall be BPSK modulated by a pseudo binary sequence to prevent the generation of spectral lines. The contribution of the pilot subcarriers to each OFDM symbol is described in the following section.

h) *Inverse Fourier Transform*

After the required spectrum is worked out, an inverse Fourier transform is used to find the corresponding time waveform. The guard period is then added to the start of each symbol. The FFT length used here is 128bits.

i) *Guard Period*

The guard period used was made up of two sections. Half of the guard period time is a zero amplitude transmission. The other half of the guard period is a cyclic extension of the symbol to be transmitted. This was to allow for symbol timing to be easily recovered by envelope detection. However, it was found that it was not required in any of the simulations as the timing could be accurately determined position of the samples. After the guard has been added, the symbols are then converted back to a serial time waveform. This is then the base band signal for the OFDM transmission.

j) *Channel*

A channel model is then applied to the transmitted signal. The model allows for the signal to noise ratio, multipath, and peak power clipping to be controlled. The signal to noise ratio is set by adding a known amount of white noise to the transmitted signal. Multipath delay spread then added by simulating the delay spread using an FIR filter. The length of the FIR filter represents the maximum delay spread, while the coefficient amplitude represents the reflected signal magnitude.

IV. RESULTS AND ANALYSIS

Four results are obtained and presented in this paper. The results show some potential and limits of using fractionally spaced equalizers and linear combiners to suppress ISI, CI, and CCI. First, with one antenna and a linear arbitrarily large receiver bandwidths allow for marginal improvements in spectral efficiency through decreased carrier spacing, because the carrier spacing cannot be reduced to a value below the symbol rate without incurring incompressible interference. Second, large receiver bandwidths assist multiple antennas in improving the spectral efficiency in that carrier spacing values may go below the symbol rate, even in the presence of CCI. Third, the use of equalizers and linear combiners, together with large receiver bandwidths, allows large transmitter bandwidths to be used. This may allow system design flexibility, e.g., constant or near-constant envelope

modulation. Fourth, for CCI and ISI, the number of interferers that may be suppressible by a generalized zero-forcing linear equalizer increases linearly with the product of the number of antennas and the truncated integer ratio of the total bandwidth to the symbol rate

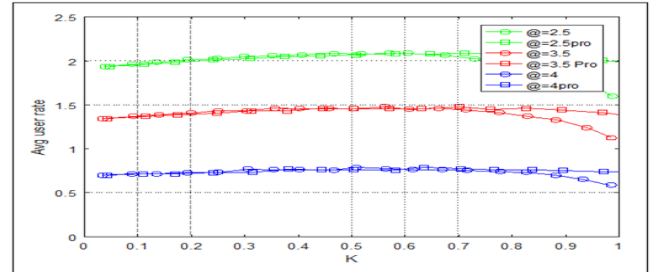


Fig 5(a) transmitter section output

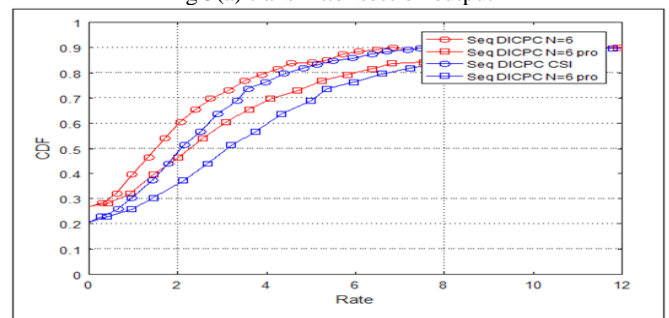


Fig 5(b) existing system output

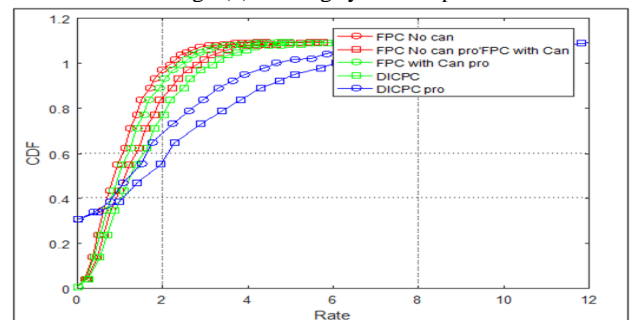


Fig 5 (c) proposed system output

load reactive power, current unbalance and current harmonics in addition to active power injection from RES. This enables the grid to supply/ receive sinusoidal and balanced power at UPF.

V. CONCLUSION

We have presented a distributed uplink power control scheme for mobile data networks that harnesses the gains from distributed interference cancellation. Numerical results show that fpc does not achieve similar performance gains when combined with interference cancellation. We have also characterized the interference prices and power updates when channel estimation errors are considered. A partial cancellation scheme was presented, which has the advantage

that the local power updates can be determined by simple closed-form expressions. A relatively simple means for partitioning users, based on power spillage to/from each user provides substantial gains in sum rate relative to a random partition. Finally, a simple heuristic was presented and analyzed for a large random network. Here, we have assumed stationary channels. The performance of DICPC with nonstationary channels is left for future work. This becomes important when different users are scheduled in successive transmission intervals. Transmitting the pilot and data symbols with different powers while constraining the power fluctuations is also an interesting topic to be explored. Furthermore, this work can be extended to account for joint scheduling across cells in addition to power control along with more general utility functions.

REFERENCES

- [1]. D. Gesbert et al., "Multi-cell MIMO cooperative networks: A new look at interference," *IEEE Journal on Selected Areas in Communications*, vol. 28, no. 9, pp. 1380–1408, December 2010.
- [2]. P. Marsch and G. P. Fettweis, *Coordinated Multi-Point in Mobile Communications: From Theory to Practice*, 1st ed. New York, NY, USA: Cambridge University Press, 2011.
- [3]. F. Boccardi, R. Heath, A. Lozano, T. Marzetta, and P. Popovski, "Five disruptive technology directions for 5G," *IEEE Communications Magazine*, vol. 52, no. 2, pp. 74–80, February 2014.
- [4]. S. Sun, Q. Gao, Y. Peng, Y. Wang, and L. Song, "Interference management through comp in 3GPP LTE-advanced networks," *IEEE Wireless Communications*, vol. 20, no. 1, pp. 59–66, February 2013.
- [5]. W. Yu, T. Kwon, and C. Shin, "Multicell coordination via joint scheduling, beamforming and power spectrum adaptation," in *2011 Proceedings IEEE INFOCOM*, April 2011, pp. 2570–2578.
- [6]. G. Li, J. Niu, D. Lee, J. Fan, and Y. Fu, "Multi-cell coordinated scheduling and MIMO in LTE," *IEEE Communications Surveys Tutorials*, vol. 16, no. 2, pp. 761–775, May 2014.
- [7]. I. Hwang, C.-B. Chae, J. Lee, and J. Heath, R.W., "Multicell cooperative systems with multiple receive antennas," *IEEE Wireless Communications*, vol. 20, no. 1, pp. 50–58, February 2013.
- [8]. O. Somekh, B. Zaidel, and S. Shamai, "Sum rate characterization of joint multiple cell-site processing," *IEEE Transactions on Information Theory*, vol. 53, no. 12, pp. 4473–4497, Dec 2007.
- [9]. M. Bacha, J. Evans, and S. Hanly, "On the capacity of MIMO cellular networks with macrodiversity," in *2006. Proceedings*.